*Inorg. Chem.* **2006**, *45*, 10750–10757


# Built-in Axial Base Binding on Phenanthroline-Strapped Zinc(II) and Iron(III) Porphyrins

**Frédéric Melin,[†] Sylvie Choua,*[,‡] Maxime Bernard,[‡] Philippe Turek,[‡] and Jean Weiss*[,†]**

*Chimie des Ligands à Architecture Contrôlée, LC3 CNRS-ULP, Institut Le Bel, 4 rue Blaise Pascal, 67070 Strasbourg Cedex, France, and Synthèse et Propriétés Optiques et Magnétiques de Matériaux Moléculaires et Macromoléculaires, Institut Charles Sadron, CNRS-UPR 22, 6 rue Boussingault, BP 40016, 67083 Strasbourg Cedex, France*

Received June 20, 2006

In addition to the need for functional models of cytochrome *c* oxidase, structural models are still required for a better understanding of the small reorganizations occurring during the catalytic cycle. An efficient synthetic approach has been designed to prepare several phenanthroline-strapped porphyrins, two of them bearing two pendant imidazoles. These built-in bases are both potentially able to act as axial bases for the metalloporphyrin and as complementary ligands for copper if necessary. Diamagnetic zinc(II) was used to demonstrate that the distal/proximal selectivity demonstrated by exogenic bases binding studies can be extended to the coordination of iron(III). Combination of EPR and paramagnetic $^1$H NMR shows that the imidazole binding on the zinc species can be further extended to the iron(III) species in dilute conditions.

## Introduction

Cytochrome *c* oxidase is the terminal enzyme of the mitochondrial respiratory chain and catalyzes the four electron reduction of dioxygen into water at low overpotentials without the formation of partial reduction byproducts.[1] The active site comprises a heme (a3) associated with a copper(I) center (CuB) coordinated by three histidine moieties, one of which is linked to a tyrosine. It has been proposed that this tyrosine residue plays a key role in the enzyme function, possibly as a relay in proton or electron transfer or as a structuring component in the environment of CuB.[2] While early functional models of cytochrome *c* oxidase were based exclusively on the reproduction of the coordination sphere of each metal in the binuclear complex,[3] a new generation of models is now emerging that incorporate a tyrosine residue cross-linked to one of the imidazoles surrounding the CuB center.[4] Despite many efforts, the elucidation of CcO's catalytic mechanism still requires both structural and functional models of the active site and eventual isolation of postulated intermediates[5] for comparison with "natural" spectroscopic data. Toward this goal, the high availability of a phenanthroline-strapped porphyrin denominated porphen (Chart 1)[6] and its ability to form bimetallic complexes[7] has prompted us to investigate its derivatization to introduce built-in imidazoles as both axial base and auxiliary copper ligand. In these ligands, the rigid character of the phenanthroline binding site may allow the stabilization of bridged Cu−Fe intermediates. We report hereafter the synthesis of two promising candidates for cytochrome *c* oxidase models that are represented in Chart 1. Only one of the imidazole moieties acts as an axial base in zinc-metalated

* To whom correspondence should be addressed. E-mail: jweiss@chimie.u-strasbg.fr (J.W.).
[†] Institut Le Bel.
[‡] Institut Charles Sadron.

(1) Fergusson-Miller, S.; Babcock, G. T. *Chem. Rev.* **1996**, *96*, 2889.
(2) Proshlyakov, D. A.; Pressler, M. A.; DeMaso, C.; Leykam, J. F.; DeWitt, D. L.; Babcock, G. T. *Science* **2000**, *290*, 1588 and references therein.
(3) (a) Collman, J. P.; Boulatov, R.; Sunderland, C. J.; Fu, L. *Chem. Rev.* **2004**, *104*, 561 and references cited. (b) Kim, E.; Chufan, E. E.; Kamaraj, K.; Karlin, K. D. *Chem. Rev.* **2004**, *104*, 1077 and references cited. (c) Naruta, Y.; Sasaki, T.; Tani, F.; Tachi, Y.; Kawato, N.; Nakamura, N. *J. Inorg. Biochem.* **2001**, *83*, 239 and references cited.
(4) (a) Liu, J.-G.; Naruta, Y.; Tani, F. *Angew. Chem., Int. Ed.* **2005**, *44*, 1836. (b) del Río, D.; Sarangi, R.; Chufán, E. E.; Karlin, K. D.; Hedman, B.; Hodgson, K. O.; Solomon, E. I. *J. Am. Chem. Soc.* **2005**, *127*, 11969. (c) Kim, E.; Kamaraj, K.; Galliker, B.; Rubie, N. D.; Moënne-Loccoz, P.; Kaderli, S.; Zuberbühler, A. D.; Karlin, K. D. *Inorg. Chem.* **2005**, *44*, 1238. (d) Collman, J. P.; Decréau, R. A.; Zhang, C. *J. Org. Chem.* **2004**, *69*, 3546. (e) Liu, J.-G.; Naruta, Y.; Tani, F.; Chisiro, T.; Tachi, Y. *Chem. Commun.* **2004**, 120.
(5) Blomberg, M. R. A.; Siegbahn, P. E.; Wikström, M. *Inorg. Chem.* **2003**, *42*, 5231.
(6) Wytko, J. A.; Graf, E.; Weiss, J. *J. Org. Chem.* **1992**, *57*, 1015.
(7) Giraudeau, A.; Gisselbrecht, J.-P.; Gross, M.; Weiss, J. *J. Chem. Soc., Chem. Commun.* **1993**, 1103.



10.1021/ic0611185 CCC: $33.50 
Published on Web 11/18/2006

**Chart 1.** Four Phenanthroline-Strapped Porphyrin Derivatives for Bimetallic Complex Formation

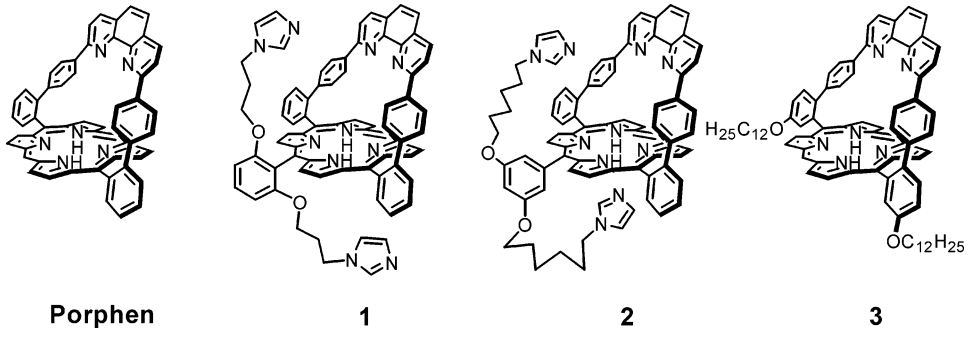


**Porphen** **1** **2** **3**

porphyrins, while the imidazole metal interaction in iron complexes appears to be concentration dependent.

## Experimental Section

All reagents and solvents were used as commercial grades, except $CH_2Cl_2$ and THF, which were distilled respectively on $P_2O_5$ and sodium/benzophenone when necessary. Melting points are uncorrected and were measured on a Kofler heating plate type 7841. $^1$H NMR spectra were recorded on Bruker Advance 500 and Advance 300 spectrometers. Chemical shifts were determined by taking the solvent as a reference: $CHCl_3$ (7.26 ppm). UV−vis spectra were performed on a Hewlett-Packard 8452A diode array spectrometer. EPR spectra were recorded with an ESP300E spectrometer (Bruker) operating at X-band and equipped with a standard rectangular cavity (TE 102). An ESR900 cryostat (Oxford Instruments) was used for low-temperature measurements down to 4 K. Samples for EPR measurements were prepared by dissolving compounds at variable concentrations in $CH_2Cl_2$/MeOH. The resulting solution was degassed by freeze−thaw pumping cycles. Chromatography columns were performed on silica gel Merck No. 7734 and alumina Merck No. 1097. 3,5-Dimethoxyphenylboronic acid[8] and *N*-(6-bromohexyl)imidazole hydrochloride[9] were prepared according to the literature.

***meso*-Bromoporphen (4).** To a solution of porphen−Zn (1 g, 1.00 mmol) in 500 mL of chloroform was added 160 mg (0.9 equiv) of *N*-bromosuccinimide. After 20 min, the reaction was quenched with 20 mL of acetone. After evaporation of the solvent, the mixture was dissolved in 200 mL of $CH_2Cl_2$ and 10 mL of trifluoroacetic acid was added. The solution was stirred for 10 min and washed twice with 2 M $Na_2CO_3$(aq). The organic layer was dried over $Na_2SO_4$, and the solvent was removed. The resulting mixture of porphyrins was purified by column chromatography over $Al_2O_3$ (neutral, activity II−III, diameter 4.5 cm, height 80 cm) in $CH_2Cl_2$/cyclohexane (50/50). Compound **3** (530 mg, 0.54 mmol, 60% yield) eluted second.

Mp: >360 °C.

$^1$H NMR ($CDCl_3$, 300 MHz): 10.00 (s, 1H), 9.58 (d, $J$ = 4.4 Hz, 2H), 9.15 (d, $J$ = 4.5 Hz, 2H), 8.84 (m, 4H), 8.69 (d, $J$ = 8 Hz, 2H), 7.99−7.84 (m, 8H), 7.53 (d, $J$ = 8 Hz, 2H) 7.49 (s, 2H), 6.77 (d, $J$ = 8 Hz, 4H), 6.48 (d, $J$ = 8 Hz, 4H), −2.69 (s, 2H).

UV−visible in $CH_2Cl_2$ [$\lambda_{max}$, nm ($\epsilon$, $M^{-1}$ $cm^{-1}$)]: 285 (70 000), 422 (260 000), 516 (16 000), 550 (5000), 592 (5000), 649 (2000).

Anal. Calcd for $C_{56}H_{33}BrN_6$ + $C_6H_{12}$ + 1/3$CH_2Cl_2$: C, 76.22; H, 4.69; N, 8.56. Found: C, 76.45; H, 4.76; N, 8.43.

***meso*-(2,6-Dimethoxyphenyl)porphen (5).** To a degassed mixture of bromoporphen (**4**) (120 mg, 0.12 mmol), 2,6-dimethoxyphenylboronic acid (50 mg, 0.28 mmol), and $K_2CO_3$ (180 mg, 1.30 mmol) in 10 mL of dry toluene was added under argon 15 mg of $Pd(PPh_3)_4$ (0.01 mmol). Another aliquot of 2,6-dimethoxyphenylboronic acid (100 mg, 0.56 mmol) was added slowly over time during the course of the reaction. After 20 h of reflux, the solvent was evaporated and the mixture was taken in 50 mL of $CH_2Cl_2$. The solution was washed twice with brine and once with water and dried over $Na_2SO_4$. Filtration and evaporation of the solvent yielded a purple solid purified by chromatography over $Al_2O_3$ (neutral, activity II−III, diameter 4 cm, height 20 cm). Elution with $CH_2Cl_2$/cyclohexane (50/50) yielded 108 mg of the porphyrin **5** (0.10 mmol, 86% yield).

Mp: >360 °C.

$^1$H NMR ($CDCl_3$, 300 MHz): 9.84 (s, 1H), 8.98 (d, $J$ = 4.7 Hz, 2H), 8.93 (d, $J$ = 4.6 Hz, 2H), 8.86 (d, $J$ = 4.9 Hz, 2H), 8.74 (d, $J$ = 7.1 Hz, 2H), 8.67 (d, $J$ = 4.6 Hz, 2H), 7.99 (d, $J$ = 8.3 Hz, 2H), 7.93−7.79 (m, 6H), 7.72 (m, 1H), 7.58 (d, $J$ = 8.3 Hz, 2H), 7.51 (s, 2H), 7.11 (d, $J$ = 9 Hz, 1H), 6.88 (m, 5H), 6.56 (d, $J$ = 8.6 Hz, 2H), 3.80 (s, 3H), 3.28 (s, 3H), −1.06 (s, 2H).

UV−visible in $CH_2Cl_2$ [$\lambda_{max}$, nm ($\epsilon$, $M^{-1}$ $cm^{-1}$)]: 285 (66 000), 421 (281 000), 514 (16 000), 548 (4000), 588 (5000), 644 (1000).

Anal. Calcd for $C_{64}H_{42}N_6O_2$ + $C_6H_{12}$ + 1/3$CH_2Cl_2$: C, 81.26; H, 5.30; N, 8.08. Found: C, 81.45; H, 5.27; N, 8.32.

***meso*-(2,6-Dihydroxyphenyl)porphen (6).** To a degassed solution of the porphyrin **5** (100 mg, 0.10 mmol) in 20 mL of freshly distilled $CH_2Cl_2$ was added dropwise, under argon, 20 mL of a 1 M solution of $BBr_3$ in $CH_2Cl_2$. The mixture was refluxed for 3 h under argon. Then 3 mL of MeOH was added. The solvents were removed, and the green solid was taken in 20 mL of dichloromethane. The solution was washed twice with 15 mL of 2 M $Na_2CO_3$(aq) and once with water and dried over $Na_2SO_4$. Filtration and evaporation of the solvent yielded 78 mg (0.08 mmol, 80%) of **6** as a red solid. This compound was used without further purification.

$^1$H NMR ($CDCl_3$, 300 MHz): 10.31 (s, 1H), 9.45 (d, $J$ = 4.6 Hz, 2H), 9.21 (d, $J$ = 4.6 Hz, 2H), 8.71 (d, $J$ = 7.0 Hz, 2H), 8.59 (m, 4H), 8.01 (d, $J$ = 8.4 Hz, 2H), 7.92 (m, 6H), 7.57 (d, $J$ = 8.4 Hz, 2H), 7.53 (s, 2H), 7.37 (t, $J$ = 8.2 Hz, 1H), 6.75−6.72 (m, 5H), 6.66 (dd, $J$ = 8.2 Hz, $J'$ = 1.1 Hz, 1H), 6.46 (d, $J$ = 8.4, 4H), −2.76 (s, 2H).

***meso*-[2,6-Bis(3-bromopropoxy)phenyl]porphen (7).** A degassed mixture of the porphyrin **6** (150 mg, 0.17 mmol), 1,3-dibromopropane (3.2 mL, 31.50 mmol), $K_2CO_3$ (250 mg, 1.81 mmol), and 18-crown-6 in 20 mL of acetone was refluxed for 20 h under argon. The solvent was evaporated, and the product was

(8) Dol, C. G.; Kamer, C. J. P.; Van Leeuwen, W. N. M. P. *Eur. J. Org. Chem.* **1998**, 359.

(9) (a) Paul, D.; Melin, F.; Hirtz, C.; Wytko, J.; Ochsenbein, P.; Bonin, M.; Schenk, K.; Maltese, P.; Weiss, J. *Inorg. Chem.* **2003**, *42*, 3779−3787. (b) Froidevaux, J.; Ochsenbein, P.; Bonin, M.; Schenk, K.; Maltese, P.; Gisselbrecht, J. P.; Weiss, J. *J. Am. Chem. Soc.* **1997**, *119*, 12362.

filtrated over $Al_2O_3/CH_2Cl_2$. Precipitation with $CH_2Cl_2$/hexane afforded 150 mg of the porphyrin **7** (0.13 mmol, 79% yield).

Mp: >360 °C.

$^1$H NMR ($CDCl_3$, 300 MHz): 9.93 (s, 1H), 9.05 (d, $J$ = 4.6 Hz, 2H), 8.91 (d, $J$ = 4.8 Hz, 2H), 8.86 (d, $J$ = 4.8 Hz, 2H), 8.70 (m, 4H), 7.97 (d, $J$ = 8.4 Hz, 2H), 7.88 (m, 6H), 7.70 (t, $J$ = 8.1 Hz, 1H), 7.54 (d, $J$ = 8.4 Hz, 2H), 7.49 (s, 2H), 7.05 (d, $J$ = 8.1 Hz, 1H), 6.99 (d, $J$ = 8.1 Hz, 1H), 6.74 (d, $J$ = 8.4 Hz, 4H), 6.50 (d, $J$ = 8.4 Hz, 4H), 4.03 (t, $J$ = 5.5 Hz, 2H), 3.93 (t, $J$ = 5.5 Hz, 2H), 2.20 (d, $J$ = 5.9 Hz, 2H), 2.11 (d, $J$ = 6.2 Hz, 2H), 1.35 (m, 4H), −2.65 (s, 2H).

UV−visible in $CH_2Cl_2$ [$\lambda_{max}$, nm ($\epsilon$, $M^{-1}$ $cm^{-1}$)]: 284 (66 000), 421 (290 000), 514 (17 000), 547 (4000), 588 (6000), 645 (1000).

Anal. Calcd for $C_{68}H_{48}Br_2N_6O_2 + 1/2C_6H_{12} + 1/2H_2O$: C, 71.54; H, 4.65; N, 7.05. Found: C, 71.23; H, 4.88; N, 7.00.

***meso*-[2,6-Bis(3-imidazol-1-ylpropoxy)phenyl]porphen (1).** To a degassed solution of imidazole (100 mg, 1.47 mmol) in 15 mL of dry THF was added, under argon, 65 mg of a 60% suspension NaH in mineral oil. When the gas evolution ceased, a solution of the porphyrin **6** (200 mg, 0.17 mmol) in 15 mL of dry THF was added dropwise under argon. The mixture was refluxed for 4 h under argon. The solvent was removed, and the green product was taken in 20 mL of dichloromethane. The solution was washed twice with 15 mL of water and dried over $Na_2SO_4$. The product was purified by chromatography over $NEt_3$-neutralized $SiO_2$ in $CH_2Cl_2$. Elution with 5% MeOH in $CH_2Cl_2$, evaporation, and precipitation with $CH_2Cl_2$/cyclohexane afforded 150 mg (0.13 mmol, 75% yield) of the porphyrin **1** as a red microcrystalline product.

Mp: >360 °C.

$^1$H NMR ($CDCl_3$, 500 MHz): 10.10 (s, 1H), 9.23 (d, $J$ = 4.6 Hz, 2H), 8.90 (d, $J$ = 4.6 Hz, 2H), 8.80 (d, $J$ = 4.6 Hz, 2H), 8.76 (d, $J$ = 4.6 Hz, 2H), 8.68 (d, $J$ = 6.4 Hz, 2H), 7.94 (d, $J$ = 8.6 Hz, 2H), 7.92−7.80 (m, 6H), 7.55 (t, $J$ = 8.3 Hz, 1H), 7.50 (s, 2H), 7.47 (d, $J$ = 8.6 Hz, 2H), 6.83 (d, $J$ = 8.3 Hz, 1H), 6.67 (d, $J$ = 8.3 Hz, 1H), 6.61 (m, 2H), 6.54 (d, $J$ = 8.4 Hz, 4H), 6.40 (d, $J$ = 8.4 Hz, 4H), 6.00 (broad s, 1H), 5.87 (s, 1H), 5.17 (broad s, 1H), 3.72 (t, $J$ = 5.3 Hz, 2H), 3.28 (m, 2H), 2.59 (t, $J$ = 6.7 Hz, 2H), 2.14 (m, 2H), 1.32 (m, 2H), 0.54 (m, 2H), −2.61 (s, 2H).

UV−visible in $CH_2Cl_2$ [$\lambda_{max}$, nm ($\epsilon$, $M^{-1}$ $cm^{-1}$)]: 285 (58 000), 419 (260 000), 513 (14 000), 546 (3000), 588 (4000), 643 (1000).

Mass spectrometry (MALDI-TOF) (*m*/*z*): mass calcd for $M + H^+$, 1115; found, 1115.0.

Anal. Calcd for $C_{74}H_{54}N_{10}O_2 + 3/5C_6H_{12}$: C, 79.95; H, 5.29; N, 12.01. Found: C, 79.69; H, 5.18; N, 11.67.

**Zn−*meso*-[2,6-Bis(3-imidazol-1-ylpropoxy)phenyl]porphen (1-Zn).** To a solution of **1** (10 mg, 0.009 mmol) in 20 mL of THF was added a 10-fold excess of $Zn(OAc)_2$ dihydrate. When the UV−visible spectrometry monitoring showed the completion of the reaction, the solvent was removed by evaporation. The crude solid was taken in $CH_2Cl_2$ and $H_2O$, washed twice with water, and dried over $Na_2SO_4$. Evaporation and precipitation with $CH_2Cl_2$/cyclohexane afforded 10 mg of the metalated porphyrin **1**-Zn (0.007 mmol, 95% yield).

$^1$H NMR ($CDCl_3$, 500 MHz): 10.10 (s, 1H), 9.31 (d, $J$ = 4.4 Hz, 2H), 8.96 (d, $J$ = 4.4 Hz, 2H), 8.74 (m, 2H), 8.61 (d, $J$ = 4.2 Hz, 2H), 8.48 (d, $J$ = 4.2 Hz, 2H), 7.93 (d, $J$ = 8.4 Hz, 2H), 7.90−7.78 (m, 6H), 7.49 (m, 3H), 7.46 (d, $J$ = 8.4 Hz, 2H), 6.83 (d, $J$ = 8.6 Hz, 1H), 6.68 (d, $J$ = 8.6 Hz, 1H), 6.54 (m, 4H), 6.45 (m, 4H), 5.76 (s, 1H), 4.95 (broad s, 1H), 3.21 (m, 4H), 2.79 (broad s, 2H), 1.26 (m, 2H), 0.37 (broad s, 2H).

**Fe−*meso*-[2,6-Bis(3-imidazol-1-yl-propoxy)phenyl]porphen (1-Fe).** To an Ar-flushed solution of **1** (100 mg, 0.09 mmol) in 30 mL of $CHCl_3$/THF (3/1) were added a large excess of $FeCl_2$ and 0.2 mL of 2,6-lutidine. The mixture was refluxed under argon for 48 h, then, the solution was filtered over cotton and the solvents were removed. The crude product was taken in $CH_2Cl_2$/EtOH (10/3), washed with water, and dried over $Na_2SO_4$. Because of its poor solubility in most common organic solvents, this compound could not be purified by column chromatography. Precipitation from $CH_2Cl_2$/EtOH/pentane afforded 50 mg of **1-Fe** as a brown-green powder (0.04 mmol, 49% yield).

Mass spectrometry (MALDI-TOF) (*m*/*z*): mass calcd for $C_{74}H_{52}N_{10}FeO_2^+$, 1168; found, 1168.39.

***meso*-(3,5-Dimethoxyphenyl)porphen (8).** To a degassed mixture of the bromoporphen (**4**) (470 mg, 0.48 mmol) in 40 mL of toluene, 3,5-dimethoxyphenylboronic acid (175 mg, 0.96 mmol) in 1.5 mL of MeOH, and $K_2CO_3$ (100 mg, mmol) in 1.6 mL of water was added 23 mg of $Pd(PPh_3)_4$ (0.02 mmol). After 24 h of reflux, the solvents were removed. The crude product was taken in 50 mL of $CH_2Cl_2$. The solution was washed twice with brine, once with water, and dried over $Na_2SO_4$. Filtration and evaporation of the solvent yielded a purple solid that was purified by chromatography over $Al_2O_3$ (neutral, activity II−III, diameter 4 cm, height 20 cm) in $CH_2Cl_2$/hexane (50/50) to afford 400 mg of the porphyrin **8** (0.43 mmol, 89% yield).

Mp: >360 °C.

$^1$H NMR ($CDCl_3$, 300 MHz): 10.13 (s, 1H), 9.29 (d, $J$ = 4.6 Hz, 2H), 9.00 (d, $J$ = 4.6 Hz, 2H), 8.76 (d, $J$ = 4.7 Hz, 2H), 8.72 (m, 2H), 8.66 (d, $J$ = 4.7 Hz, 2H), 7.97−7.82 (m, 8H), 7.79 (s, 1H), 7.51 (d, $J$ = 8.4 Hz, 2H), 7.45 (s, 2H), 7.01 (s, 1H), 6.81−6.72 (m, 5H), 6.50 (d, $J$ = 8.6 Hz, 2H), 3.80 (m, 6H), −2.70 (s, 2H).

UV−visible in $CH_2Cl_2$ [$\lambda_{max}$, nm ($\epsilon$, $M^{-1}$ $cm^{-1}$)]: 284 (69 000), 310 shoulder, 420 (310 000), 513 (17 000), 546 (4000), 587 (5000), 642 (1000).

Anal. Calcd for $C_{64}H_{42}N_6O_2 + 1/2H_2O$: C, 82.12; H, 4.63; N, 8.98. Found: C, 81.96; H, 5.09; N, 9.50.

***meso*-(3,5-Dihydroxyphenyl)porphen (9).** To a degassed solution of the porphyrin **8** (400 mg, 0.43 mmol) in 30 mL of freshly distilled $CH_2Cl_2$ was added dropwise, under argon, 20 mL of a 1 M solution of $BBr_3$ in $CH_2Cl_2$. After 3 h of reflux, 10 mL of MeOH was added. The solvents were removed, and the green product was taken in 20 mL of $CH_2Cl_2$. The solution was washed twice with 15 mL of 2 M $Na_2CO_3$(aq), once with water, and dried over $Na_2SO_4$. Evaporation of the solvent afforded 390 mg (0.41 mmol, ca. 95%) of **8** as a red microcrystalline product. This compound was used without further purification.

$^1$H NMR ($CDCl_3$, 300 MHz): 10.10 (s, 1H), 9.26 (d, $J$ = 4.8 Hz, 2H), 8.96 (d, $J$ = 4.8 Hz, 2H), 8.74−8.66 (m, 4H), 8.63 (d, $J$ = 4.6 Hz, 2H), 7.96−7.80 (m, 8H), 7.50 (s, 1H), 7.43 (d, $J$ = 8.1 Hz, 2H), 7.35 (s, 2H), 6.74 (s, 1H), 6.69 (d, $J$ = 8.0 Hz, 4H), 6.52 (s, 1H), 6.45 (d, $J$ = 8.0 Hz, 4H), −2.81 (s, 2H).

***meso*-[3,5-Bis((6-imidazol-1-yl-hexyl)oxy)phenyl]porphen (2).** A degassed mixture of the porphyrin **9** (390 mg, 0.43 mmol), $K_2CO_3$ (1 g, 7.24 mmol), and *N*-(6-bromohexyl)imidazole hydrochloride (347 mg, 1.3 mmol) in 50 mL of DMF was heated under argon at 40 °C for 48 h. After removal of the solvent, the crude product was redissolved in $CH_2Cl_2$ and washed twice with water. The solution was dried over $Na_2SO_4$, and the solvent was removed. The red product was purified by column chromatography over $Al_2O_3$. Elution with 5% EtOH in $CH_2Cl_2$, evaporation, and precipitation with $CH_2Cl_2$/cyclohexane afforded 270 mg (0.22 mmol, 51% yield) of the porphyrin **2** as a red microcrystalline product.

$^1$H NMR ($CDCl_3$, 500 MHz): 10.13 (s, 1H), 9.29 (d, $J$ = 4.5 Hz, 2H), 8.99 (d, $J$ = 4.5 Hz, 2H), 8.74 (d, $J$ = 5 Hz, 2H), 8.73 (m, 2H), 8.64 (d, $J$ = 4.5 Hz, 2H), 7.95 (d, $J$ = 8.5 Hz, 2H), 7.85

(m, 6H), 7.73 (s, 1H), 7.52 (d, $J$ = 8.5 Hz, 2H), 7.48 (s, 2H), 7.42 (s, 1H), 7.30 (s, 1H), 6.99 (s, 1H), 6.95 (m, 2H), 6.82 (s, 1H), 6.75 (d, $J$ = 8.5 Hz, 4H), 6.73 (s, 1H), 6.69 (s, 1H), 6.47 (d, $J$ = 8.5 Hz, 2H), 4.48 (broad s, 1H), 3.95 (m, 4H), 3.85(t, $J$ = 7 Hz, 2H),3.66 (t, $J$ = 7 Hz, 2H), 1.72−1.18 (m, 16H), −2.72 (s, 2H).

UV−visible in $CH_2Cl_2$ [$\lambda_{max}$, nm ($\epsilon$, $M^{-1}$ $cm^{-1}$)]: 284 (60 000), 310 shoulder (55 000), 420 (269 000), 513 (14 000), 546 (5000), 587 (3000), 643 (1000).

Mass spectrometry (MALDI-TOF) (*m*/*z*): mass calcd for M + $H^+$, 1199; found, 1198.9.

Anal. Calcd for $C_{80}H_{66}N_{10}O_2 + 1/2CH_2Cl_2$: C, 77.85; H, 5.44; N, 11.28. Found: C, 77.84; H, 5.79; N, 11.53.

**Zn−*meso*-[3,5-Bis((6-imidazol-1-yl-hexyl)oxy)phenyl]porphen (2-Zn).** To a solution of **2** (10 mg, 0.008 mmol) in 20 mL of THF was added a 10-fold excess of $Zn(OAc)_2$ dihydrate. When the UV−visible spectrometry monitoring showed the completion of the reaction, the solvent was removed by evaporation. The crude solid was taken in $CH_2Cl_2$ and $H_2O$, washed twice with water, and dried over $Na_2SO_4$. Evaporation and precipitation with $CH_2Cl_2$/cyclohexane afforded 9 mg of the metalated porphyrin **2**-Zn (0.007 mmol, 85% yield).

$^1$H NMR ($CDCl_3$, 500 MHz): 10.03 (s, 1H), 9.29 (d, $J$ = 4.5 Hz, 2H), 8.95 (d, $J$ = 4.5 Hz, 2H), 8.72 (d, $J$ = 7.5 Hz, 2H), 8.64 (d, $J$ = 4.5 Hz, 2H), 8.56 (d, $J$ = 4.5 Hz, 2H), 7.94 (d, $J$ = 8.5 Hz, 2H), 7.88−7.78 (m, 7H), 7.53 (d, $J$ = 8.5 Hz, 2H), 7.47 (s, 2H), 7.46 (s, 1H), 7.04 (s, 1H), 6.75 (d, $J$ = 8.5 Hz, 4H), 6.65 (s, 1H), 6.58 (s, 1H), 6.44 (d, $J$ = 8.5 Hz, 4H), 4.99 (s, 1H), 4.00 (t, $J$ = 6.5 Hz, 2H), 3.94 (m, 2H), 3.63 (m, 2H), 2.58 (m, 2H), 2.35 (s, 1H), 2.16 (s, 1H), 1.67 (m, 2H), 1.54 (m, 4H), 1.35 (m, 2H), 1.17 (m, 2H), 0.95 (m, 2H), 0.74 (m, 2H), 0.28 (m, 2H).

**Fe−*meso*-[3,5-Bis((6-imidazol-1-yl-hexyl)oxy)phenyl]porphen (2-Fe).** To an Ar-flushed solution of **2** (130 mg, 0.10 mmol) in 30 mL of $CHCl_3$/THF (3/1) were added a large excess of $FeCl_2$ and 0.2 mL of 2,6-lutidine. The mixture was refluxed under argon for 48 h; then the solution was filtered over cotton and the solvents were removed. The crude product was taken in $CH_2Cl_2$/EtOH (10/3), washed with water, and dried over $Na_2SO_4$. Because of its poor solubility in most common organic solvents, this compound could not be purified by column chromatography. Precipitation from $CH_2Cl_2$/EtOH/pentane afforded 75 mg of **2**-Fe as a brown powder (0.06 mmol, 58% yield).

Mass spectrometry (MALDI-TOF) (*m*/*z*): mass calcd for $C_{80}H_{64}N_{10}FeO_2^+$, 1252; found, 1251.89.

**Fe−Didodecanoxyporphen (3-Fe).** To an Ar-flushed solution of **3**[12] (140 mg, 0.12 mmol) in 15 mL of THF distilled over sodium/benzophenone were added a large excess of $FeCl_2$ and 0.2 mL of 2,6-lutidine. The mixture was refluxed under argon for 24 h. The solvent was removed, and the crude product was taken in $CH_2Cl_2$, filtrated over Celite, and washed twice with 4 M HCl(aq). The solution was dried with $Na_2SO_4$, and the ferric porphyrin was purified by column chromatography over $Al_2O_3/CH_2Cl_2$. The solution was then saturated with HCl vapors. Evaporation of the solvent afforded 80 mg of a brown powder (0.06 mmol, 50% yield).

Anal. Calcd for $C_{80}H_{80}ClFeN_6O_2 + CH_2Cl_2$: C, 72.94; H, 6.20; N, 6.30. Found: C, 72.80; H, 6.51; N, 5.92.

Mass spectrometry (MALDI-TOF) (*m*/*z*): mass calcd for $C_{80}H_{80}FeN_6O_2$, 1212, and for $C_{80}H_{80}ClFeN_6O_2 + H^+$, 1248; found, 1212.260 (intensity 100%), 1248.150 (intensity 36%).

(10) Montanari, F.; Penso, M.; Quici, S.; Vigano, P, *J. Org. Chem.* **1985**, *50*, 4888.
(11) Weyermann, P.; Diederich, F. *Helv. Chim. Acta* **2002**, *85*, 599.
(12) Weyermann, P.; Diederich, F.; Gisselbrecht, J.-P.; Boudon, C.; Gross, M. *Helv. Chim. Acta* **2002**, *85*, 571.

**Scheme 1** [a]

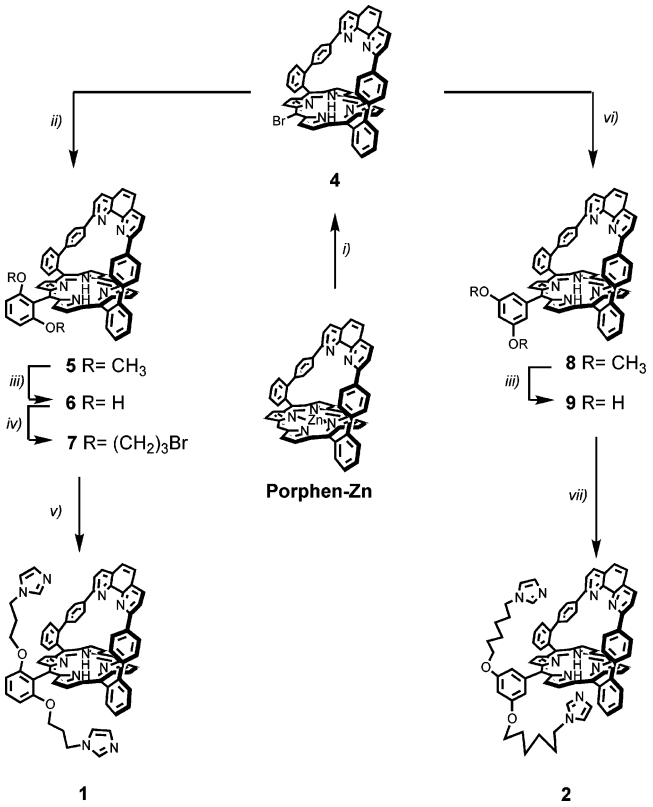


[a] Key: (i) (a) NBS 0.9 equiv, $CHCl_3$, 0 °C; (b) excess $CF_3COOH$, rt, $CH_2Cl_2$, 60%; (ii) excess 2,6-dimethoxyphenylboronic acid, $K_2CO_3$, $Pd(PPh_3)_4$, toluene, 80 °C, 86%; (iii) $BBr_3$, $CH_2Cl_2$, reflux, quant; (iv) 1,3-dibromopropane, $K_2CO_3$, 18-crown-6, acetone, reflux, 79%; (v) imidazole, NaH, THF, reflux, 75%; (vi) 3,5-dimethoxyphenylboronic acid, $K_2CO_3$, $Pd(PPh_3)_4$, MeOH/$H_2O$/toluene, reflux, 89%; (vii) *N*-(6-bromohexyl)imidazole hydrochloride, $K_2CO_3$, DMF, 40 °C, 51%.

## Results and Discussion

**Synthesis.** The phenanthroline-strapped porphyrin was halogenated with substoichiometric amounts of *N*-bromosuccinimide in chloroform in 69% yield by analogy with described procedures.[9] The corresponding bromide could then be utilized as a starting material for anchoring functional groups at the periphery of the porphyrin ring. Attempts to develop convergent approaches using imidazole functionalized resorcinol to couple to the halide **4** for the synthesis of our target ligands failed, mainly because of the generation of byproducts resulting from lithiation on the alkyl imidazole rings. Thus, we proceeded according to Scheme 1, starting from a strapped porphyrin **4** which was coupled under modified (ii) or classical (vi) Suzuki conditions with boronic acid derivatives of resorcinol dimethyl ethers to provide the dimethyl ethers **5** and **8** in respectively 86 and 89% yield. Surprisingly, classical conditions applied to the preparation of **5** were unsuccessful, as was the utilization of modified conditions in the case of **8**. In the first case, only reduced starting material was recovered at the end of the reaction, while, in the latter case, no reaction was observed. Steric hindrance surrounding the boronic acid functionality on 2,6-dimethoxyphenylboronic acid possibly explains a low efficiency for the coupling reaction that generates **5**. Steric hindrance allows the palladated intermediates to react with traces of water during the synthesis of **5**. Thus, the use of

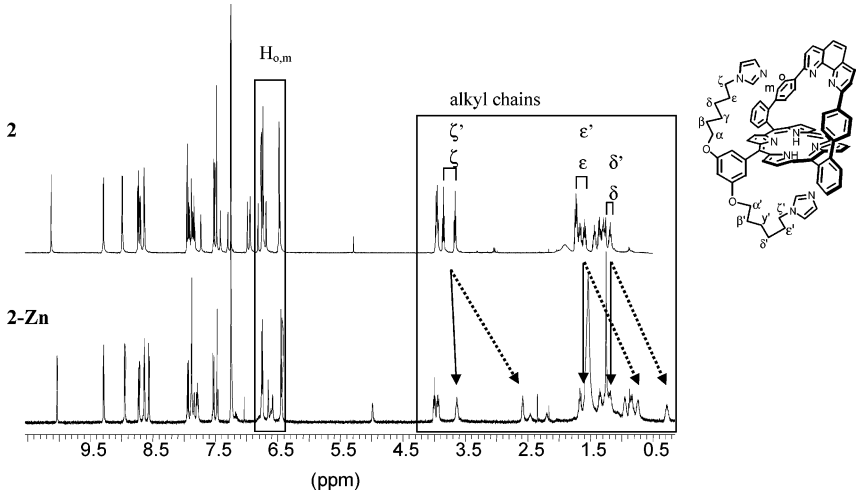


**Figure 1.** $^1$H NMR evolution upon zinc(II) insertion in ligand **2** [$CDCl_3$ (300 MHz) at 298 K].

totally anhydrous conditions was necessary, and prior to their use in modified Suzuki conditions, traces of water in the starting materials were removed by toluene/water azeotrope distillation. Toluene was added to the bromo derivative **4** and removed in a vacuum three times. The third time, only half of the toluene was evaporated and the remaining dry mixture was used for the coupling reaction. The ethers were subsequently cleaved with boron tribromide in quantitative yield to produce the corresponding dihydroxylated species **6** and **9**, which were used as crude material for the next step. The alkylation of **9** was rather straightforward due to the availability of *N*-(6-bromohexyl)imidazole hydrochloride,[10] which can be used in slight excess in the presence of $K_2CO_3$ to generate the desired ligand **2** in moderate yield (51%). On the contrary, the introduction of a short hydrocarbon linkage between the pendant imidazoles and the resorcinol moiety first required incorporation of a bromopropyl ether on the hydroxyl functions of **6** and then substitution of the pendant dibromide groups of **7** with imidazole under basic conditions.

**Zinc Coordination in Ligands 1 and 2.** Prior to any studies involving paramagnetic iron(III) porphyrins, it was necessary to estimate the ability of the ligand's proximal (open face) built-in axial base to coordinate the central metal core. Comparison of UV−visible absorption of porphen−Zn reference compound with the zinc(II) complexes **1**-Zn and **2**-Zn clearly shows red-shifted absorptions that are typical of axial coordination of the zinc central atom. Intuitively, it was expected that only the proximal imidazole would bind to the central metal, and this assumption, in part, led to the design of **1** and **2**. However, direct proof of an exclusive proximal binding was required to confirm that the distal imidazole moiety remains available for copper(II/I) coordination in synergy with the phenanthroline chelate. Extrapolation of zinc(II) binding properties to high-spin iron(III) properties is usual in the case of a single built-in axial ligand.[11] However, the behavior of iron species based on pentacoordinated zinc models in which two identical built-in axial bases are present is more difficult to anticipate, unless both faces of the porphyrin ring are equivalent.[12] Indeed, extrapolation of the unusual porphen−Zn behavior in the presence of imidazoles demonstrated in earlier work[9] would have suggested the exclusive formation of pentacoordinated iron(III) complexes in the presence of *N*-methylimidazole that is unable to bind porphen−Zn on its distal side. Thus, one- and two-dimensional NMR experiments were performed on both ligands as free bases and on their respective zinc complexes **1**-Zn and **2**-Zn. These experiments are conclusive regarding the similar nature of the axial binding to the central zinc atom but also point out a drastic difference in the behavior of **1**-Zn and **2**-Zn due to the respective presence and absence of atropoisomerism.

The NMR signatures of **2** and **2**-Zn are represented in Figure 1. The free ligand (upper trace), shows that the symmetrical character of the phenanthroline moiety remains unaffected by the disymmetry introduced on the porphyrin ring. This is not necessarily expected for the phenyl spacers whose rotation could have been precluded by insertion of the imidazole in the lipophillic cavity defined by the strap. Using COSY and ROESY experiments carried out on the free base **2** and starting from an arbitrary assignment of $H_i$ and $H_j$, assignment was made of signals corresponding to connected $CH_2$ groups of the alkyl chains (see Supporting Information). Both alkyl chains are exchangeable on the NMR time scale of the 2D experiments, which is confirmed by chemical exchange correlations observed in the ROESY spectrum. In the 1D spectrum, the two alkyl chains give distinct signals and are thus not exchangeable on the 1D NMR time scale at 500 MHz. The assignment of signals corresponding to the phenanthroline strap itself is straightforward and has been already discussed previously.[9]

Upon zinc insertion (Figure 1, bottom), only the portion corresponding to the alkyl chains is clearly perturbed. It is anticipated that only the chain bearing the imidazole bound to the zinc will be affected, as zinc porphyrins usually form pentacoordinated complexes in solution. It has been demonstrated in the past that when imidazole binding occurs within the strap, the phenyl spacer's protons $H_{o,m}$ show significant shielding due to the imidazole ring current. The fact that no chemical shift displacements are observed for the protons $H_{o,m}$ indicates that imidazole binding takes place on the unencumbered proximal face of the strapped porphy-

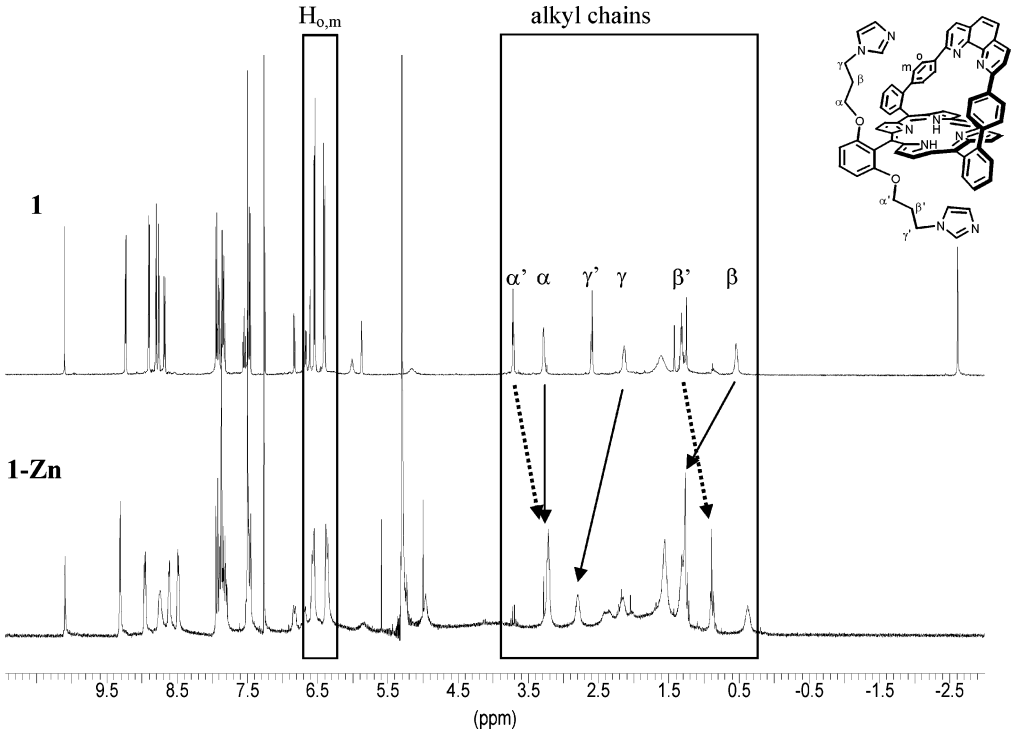


**Figure 2.** $^1$H NMR evolution upon zinc(II) insertion in ligand **1** [$CDCl_3$ (300 MHz) at 298 K].

rin. The ROESY experiment performed on **2**-Zn (see Supporting Information) shows that, on the NMR time scale, the imidazole bound to the zinc does not suppress the free rotation of the resorcinol substituent, because chemical exchange correlations are still observed between each group of protons located on the alkyl chains bearing the imidazoles.

In the case of **1** and **1-Zn** displayed in Figure 2, the behavior is similar, except that the atropoisomery is confirmed by the absence of chemical exchange correlations between the alkyl chains protons in both the free base **1** and the zinc complex. Upon zinc insertion (Figure 2), one set of signals corresponding to alkyl chain protons is clearly broadened. Again, no changes are observed for the phenyl spacer protons, which suggests that binding takes place on the unhindered face of the ligand. It should be noted that the alkyl chain signals that remain unchanged going from **2** to **2**-Zn, and almost unchanged from **1** to **1**-Zn by the zinc insertion, are initially more shielded, which suggests that the alkyl chain on the distal side is subject to the ring current of the phenanthroline plane. With a short alkyl linker between the resorcinol moiety and the imidazole, the broadening of the alkyl chain protons results mostly from motion restriction upon binding.

Thus, both ligands **1** and **2** are suitable to generate five coordinate zinc(II) models for heme proteins, and the presence of three available nitrogen atoms on the distal site should allow the insertion of copper(II/I) in the phenanthroline strap.

Contrary to imidazole-binding studies performed with zinc(II) species, classical UV−visible experiments were not helpful in establishing whether the coordination of *N*-methylimidazole in the strap is precluded for steric reasons or if the iron(III) porphyrins **1** and **2** form hexacoordinated species. While zinc(II) porphyrins have exclusively shown proximal coordination of *N*-alkylimidazoles so far, iron(III) porphyrins usually show an enhanced affinity for the second imidazole to produce hexacoordinated low-spin iron(III) complexes. Thus, the extrapolation of the zinc(II) porphyrin behavior required validation rather than assumption, and built-in imidazole proximal coordination has been investigated. Iron(III) complexes designed as hemelike molecular compounds have been much studied through EPR spectroscopy.[13] To assess their spin state, EPR measurements were performed on both iron(III) complexes of ligands **1** and **2**. In addition, EPR experiments in the presence of *N*-methylimidazole were performed on the iron(III) complex of compound **3**, which was previously described as the most soluble ligand in the phenanthroline-strapped porphyrin series.[14] For comparison, complementary experiments using paramagnetic NMR on the soluble **3**-Fe complex were also performed to study imidazole binding at room temperature for comparison.

EPR measurements on **1**-FeCl and **2**-FeCl were performed at 4.2 K in $CH_2Cl_2$/MeOH (4/1) frozen solutions to obtain a fairly good resolution of the signals. The top trace in Figure 3 shows the EPR spectrum of **1**-FeCl, and *g* values are reported in Table 1. A similar spectrum is obtained with **2**-FeCl with slightly different *g* values. The last column of Table 1 yields int (%) values as the contribution of the $S = 3/2$ spin state in the admixed ($S = 5/2, 3/2$) intermediate-spin state.[15] Low values indicate a pentacoordinated species with a quite pure, high-spin state ($S = 5/2$) iron(III)

(13) Walker, F. A. *Chem. Rev.* **2004**, *104*, 589.
(14) Koepf, M.; Melin, F.; Jaillard, J.; Weiss, J. *Tetrahedron Lett.* **2005**, *46*, 139.
(15) Sakai, T.; Ohgo, Y.; Hoshino, A.; Ikeue, T.; Saitoh, T.; Takahashi, M.; Nakamura, M. *Inorg. Chem.* **2004**, *43*, 5034.

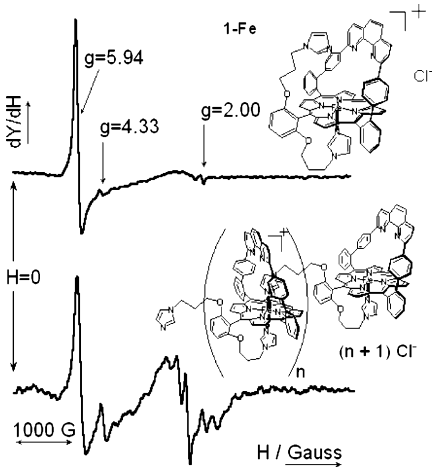


**Figure 3.** EPR (X band) spectra of **1**-FeCl at $10^{-4}$ M concentration (top trace) and $5 \times 10^{-3}$ M (lower trace) in frozen $CH_2Cl_2$ at 4.2 K.

**Table 1.** EPR Spectra at 4.2 K

| compd | $g_1$ | $g_2$ | $g_3$ | int (%)[a] |
|---|---|---|---|---|
| **1-FeCl**[b] | 5.94 | 5.94 | 2.00 | 1 |
| **2-FeCl**[c] | 6.37 | 5.40 | 2.01 | 5.8 |
| **3-FeCl**[d] | 5.95 | 5.95 | 1.99 | |
| **3-FeCl**[e] | 5.93 | 3.82 | 3.16 | 2.5 |

[a] Int (%) = $[(6.0 - g_-)/2] \times 100$.[15] [b] $CH_2Cl_2$/MeOH (4:2). [c] $CH_2Cl_2$/MeOH (6:4). [d] In the solid state [e] In $CH_2Cl_2$.

configuration. The weak signal at $g = 4.3$, which is more intense for **2**-FeCl, may be assigned to non-heme iron(III)[16a] or to an intermediate $S = 3/2$ spin state with rhombic symmetry.[16b] Its weakness and the lack of additional well-resolved peaks does not allow for a precise assignment.

As the concentration of **1**-FeCl was increased up to $5 \times 10^{-3}$ M, new lines are observed around $g = 2.00$ (Figure 3). These reveal the presence of the low-spin ($S = 1/2$) iron(III) configuration even though high-spin pentacoordinated iron(III) species are still observable. Such a mixture has been attributed to the formation of coordination oligomers through intermolecular binding of the second built-in base in the distal coordination site,[17] and spectral signatures that may originate from the same phenomenon have been described.[18] The behavior of **2**-FeCl is very similar to that for **1**-FeCl although due to its higher solubility, high-spin species are observed at concentrations up to $10^{-3}$ M in $CH_2Cl_2$/MeOH (3/2) of **2**-FeCl (see Supporting Information).

The EPR spectra of **3**-FeCl have also been analyzed (Table 1). Although the complex exhibited a high-spin state ($S = 5/2$) in the solid state, it showed the admixed intermediate-spin state ($S = 5/2, 3/2$) in $CH_2Cl_2$ solution, as revealed by the shift of the perpendicular component of the high-spin state signal toward higher field, together with the broad signal at $g \sim 3.1$. Such solvent effects have been previously reported and discussed in pentacoordinated iron(III) porphyrin complexes.[15] A "large-$g_{max}$" feature (type I EPR signal)[13] is also observed at $g = 3.80$ in the pure compound, supporting the presence of low spin ($S = 1/2$). Such a broad line has been assigned to axial ligands in a range of tilt angles around mutually perpendicular planes, combined with some microheterogeneity.[13] The starting state in solution should then be seen as a mixture of various coordination schemes leading to the coexistence of different ground spin states. Considerable solubility of **3**-FeCl in organic solvents made it possible to follow the evolution of the EPR spectra upon addition of *N*-methylimidazole. In the presence of 1 equiv of imidazole, a low-spin ($S = 1/2$) hexacoordinated species was also observed at $g = 2.95$, $g = 2.35$, and $g = 1.49$, in addition to the high-spin pentacoordinated species. Due to the scaling, this latter high-field feature is not clearly seen in Figure 4. At higher concentrations of *N*-methylimidazole, the previously discussed $g = 4.33$ weak peak was observed. The broad hump on the low field side of the $g = 2.95$ peak may be the evolution of the "large-$g_{max}$" feature between $g = 3.80$ and ca. 3.30, in agreement with the origin of this feature. Complete disappearance of the pentacoordinated signal at $g = 5.93$ required the addition of 16 equiv of *N*-methylimidazole to **3**-FeCl. This suggests that the binding of the imidazole in the distal coordination site is still disfavored, and it explains the mixture of hexa- and penta-coordinated species observed for ligands bearing built-in bases.

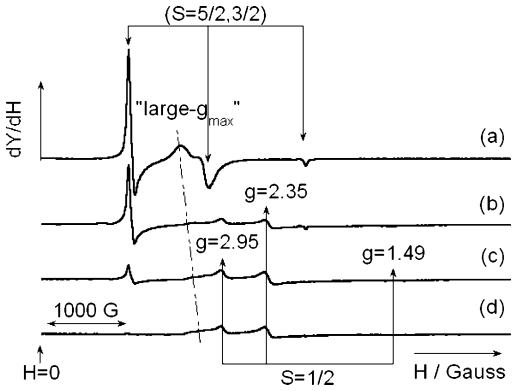


**Figure 4.** EPR spectra of **3**-FeCl at $10^{-4}$ M concentration in the presence of increasing amounts of imidazole (*N*-MeIm) in frozen $CH_2Cl_2$ at 4.2 K: (a) pure **3**-Fe; (b) **3**-Fe + *N*-MeIm (1 equiv); (c) **3**-Fe + *N*-MeIm (2 equiv); **3**-Fe + *N*-MeIm (10 equiv). All spectra are scaled at the same spectrometer settings.

However, this effect of the strap remains hypothetical as it is known that binding of 1 or 2 exogenic *N*-Me-imidazoles at concentrations in the $10^{-3}$ M range require an excess of imidazole.[19] It is thus possible that the observed high-spin species correspond to residual **3**-FeCl and that binding of imidazole leads directly to the hexacoordinated species. Still, the behavior of **3**-FeCl in the presence of excess *N*-MeIm explains the origin of low-spin species observed for **1**-FeCl at $5 \times 10^{-3}$ M. The NMR spectrum of **3**-FeCl in the presence of 16 equiv of *N*-methylimidazole is represented in Figure 5, and all possible assignments have been confirmed by COSY experiments (see Supporting Information). NMR

(16) (a) Yatsunyk, L. A.; Shokhirev, N. V.; Walker, F. A. *Inorg. Chem.* **2005**, *44*, 2848. (b) Yatsunyk, L. A.; Walker, F. A. *Inorg. Chem.* **2004**, *43*, 757.
(17) Collman, J. P.; Braumau, J. L.; Doxsee, K. M.; Halbert, T. R.; Bunneberg, E.; Linder, R. E.; La Mar, G. N.; Del Gaudio, J.; Lang, G.; Spartalian, K. *J. Am. Chem. Soc.* **1980**, *102*, 4182.
(18) Walker, F. A.; Reis, D.; Balke, V. L. *J. Am. Chem. Soc.* **1984**, *106*, 6888.
(19) Walker, F. A.; Lo, M.-W.; Ree, M. T. *J. Am. Chem. Soc.* **1976**, *98*, 5552.

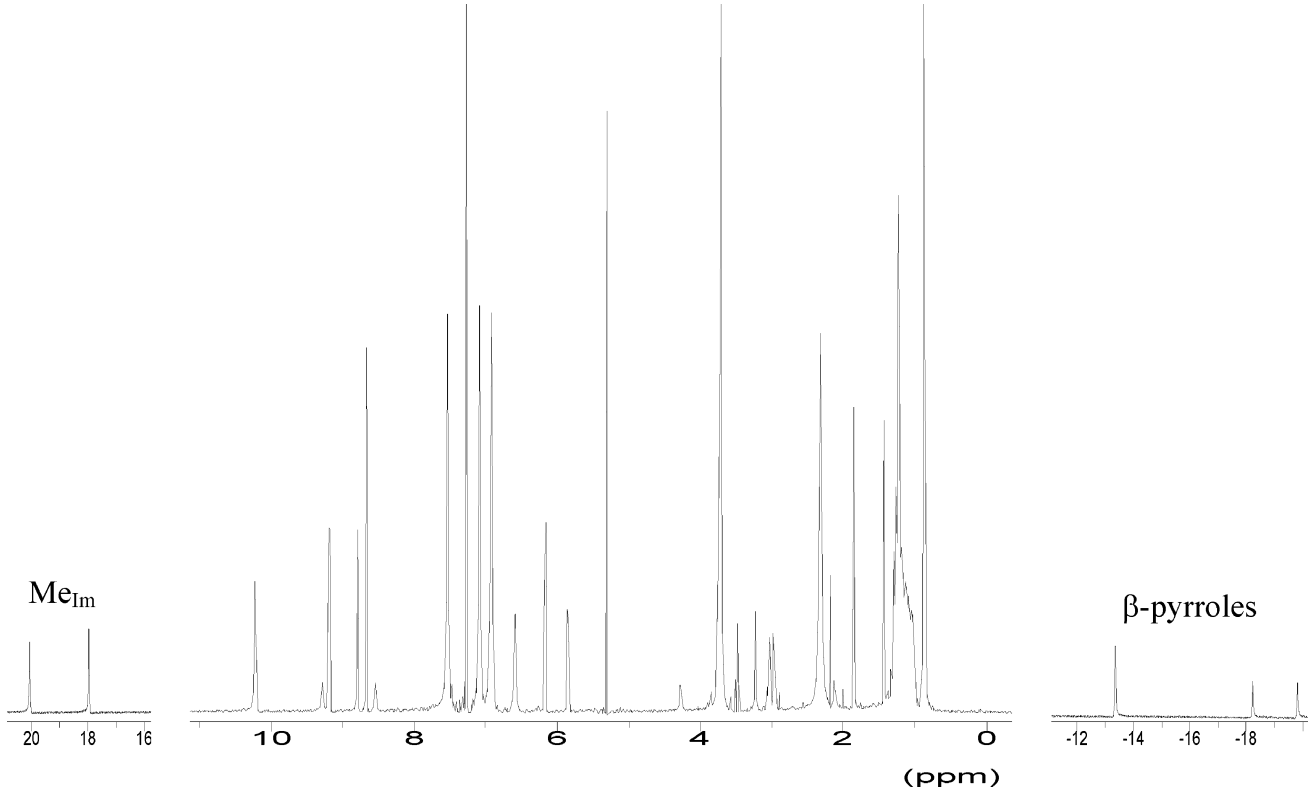


**Figure 5.** $^1$H NMR spectrum of low-spin paramagnetic **3**-FeCl in the presence of 16 equiv of *N*-methylimidazole in $CD_2Cl_2$ at 298 K (300 MHz).

clearly shows the shielded $\beta$ pyrrolic protons and therefore confirms the $(d_{xy})^2(d_{xz}, d_{yz})^3$ configuration of the hexacoordinated iron(III). Additionally, two distinct signals are observed for the two *N*-methyl substituents on the axial imidazole ligands, which suggests that the exchange of the axial bases with free imidazole in solution is slow on the NMR time scale, which contrasts with observations reported for FeTPPCl.[20]

## Conclusion

These results show that the selectivity observed in the coordination of imidazoles in phenanthroline-strapped zinc(II) porphyrin can be extended to the corresponding iron complexes in the case of strapped porphyrins bearing built-in bases in dilute conditions. The selective binding of imidazole on the open face of the strapped porphyrin reproduces the proximal coordination observed in cytochrome *c* oxidase, and similarly to the behavior of the corresponding zinc(II) porphyrins, the second *N*-alkylimidazole does not bind to the central metal core. However, in concentrations exceeding $10^{-4}$ M in organic solvents, the binding of a sixth ligand, which is favored by ligand field effects, cannot be prevented by the phenanthroline strap and hexacoordinated low-spin iron(III) complexes are formed. The new phenanthroline-strapped ligands comprising built-in bases described in this work are good candidates as functional models of cytochrome *c* oxidase. Electrocatalytic studies of oxygen reduction with both the iron and the iron−copper complexes by analogy with cytochrome *c* oxidase are under progress, and results will be published elsewhere.

**Acknowledgment.** The Centre National de la Recherche Scientifique (CNRS) and the Université Louis Pasteur are acknowledged for financial support. F.M. thanks the Ministère de l'Education Nationale, Recherche et Technologie (MENRT) for a Ph.D. fellowship.

**Supporting Information Available:** ROESY spectra of **1**, **2**, **1**-Zn, and **2**-Zn, an expanded view of the 1−4 ppm area of the COSY spectrum of **2**, the 0−4 ppm ROESY spectrum of **2**-Zn, and EPR data for [**2**-Fe]Cl at $10^{-4}$ M. This material is available free of charge via the Internet at http://pubs.acs.org.

IC0611185

(20) (a) Scheidt, W. R.; Reed, C. A. *Chem. Rev.* **1981**, *81*, 543. (b) Walker, F. A. In *The Porphyrin Handbook*; Academic Press: New York, 2000; Vol. 5, p 81.